Back-bonding between an electron-poor, high-oxidation-state metal and poor π-acceptor ligand in a uranium(v)–dinitrogen complex

Erli Lu, Benjamin E. Atkinson, Ashley J. Wooles, Josef T. Boronski, Laurence R. Doyle, Floriana Tuna, Jonathan D. Cryer, Philip J. Cobb, Inigo J. Vitorica-Yrezabal, George F. S. Whitehead, Nikolas Kaltsoyannis, and Stephen T. Liddle*

School of Chemistry, The University of Manchester, Oxford Road, Manchester, M13 9PL, UK.

*Email: steve.liddle@manchester.ac.uk

Abstract

A fundamental bonding model in coordination and organometallic chemistry is the synergic, donor-acceptor interaction between a metal and neutral π-acceptor ligand where the ligand σ-donates to an electron-rich, mid, low, or even negative, oxidation state metal which π-backbonds to a π-ligand orbital. Here, we report that treatment of a uranium-carbene complex with an organo-azide produces an isolable, crystalline uranium(V)-bis(imido)-dinitrogen-complex. This is an unknown functional group transformation for metal-carbenes, and this complex violates the classical donor-acceptor bonding model since it involves an electron-poor, high oxidation state uranium(V) $5f^1$ ion π-backbonded to dinitrogen. This electron-poor backbonding could have implications for the field of dinitrogen activation chemistry, and suggests that an established model of metal-ligand bonding can be subverted when metals are coordinated to very electron-rich ancillary ligands.*

Introduction

In coordination and organometallic chemistry, a well-established fundamental bonding model is that neutral π-acceptor ligands, such as isoelectronic dinitrogen (N_2) and carbon monoxide (CO), can ligate end-on to metals in a synergic donor-acceptor interaction.[1] In this classical bonding model σ-donation from the ligand lone pair to the metal is complemented by metal π-backbonding to a formally vacant π* acceptor molecular orbital of the ligand resulting in weak ligand activation, Fig. 1. It naturally follows that in order to engage in metal-to-ligand backbonding a key requirement is that the metal must be in a medium to low, or even negative, formal oxidation state so that it is sufficiently electron-rich to possess the requisite valence electrons for backbonding. An inherent consequence of this scenario is that a low oxidation state metal centre will exhibit more radially extended valence orbitals compared to higher oxidation states, thus enabling effective spatial overlap with the ligand π* orbitals. Thus, a high oxidation state and electron-poor metal is usually inherently ill-suited, if not incapable, of engaging in π-backbonding to π-acceptor ligands.

For N_2 complexes, although $[U(N)_2(N_2)_n]$ (n = 1-5) species formally containing uranium in oxidation state +VI have been spectroscopically detected when trapped under cryogenic matrix isolation conditions,[2,3] no classical molecular N_2-complex isolable on macroscopic scale is known beyond a metal oxidation state of +III, otherwise strong activation to give reduced N_2^{n-} (n = 2, 4) with high oxidation state metals occurs.[3,4] CO is a better π-acceptor ligand than N_2, so metal oxidation state +IV but electron-rich carbonyl anions such as $[PtCl_5(CO)]^{1-}$, $[OsF_5(CO)]^{1-}$, $[OsCl_5(CO)]^{1-}$ are known,[5-7] yet despite the fact these M(IV) ions are electron-rich they are exceedingly rare and only the latter is structurally authenticated.[7] Transient or matrix isolation-trapped M(IV) $[M(O)_2(CO)_n]$ (M = Rh, n = 1; M = Mo, W, n = 4) species have been detected spectroscopically,[8,9] and the formally +VI osmium dication $[OsO_2(CO)_4]^{2+}$ has been reported, but was too unstable to be isolated and fully characterised.[10] Very recently the Fe(IV) dication $[Fe(\eta^5\text{-}C_5Me_5)_2(CO)]^{2+}$ was structurally authenticated,[11] but is stabilised via C_5Me_5-to-CO ligand-to-ligand

π-backbonding. This bonding type is a departure from the classical model, and appears to be unique to metallocene complexes, being similarly proposed for d^0 M(IV) [M(η^5-C_5Me_5)$_2$(H)$_2$(CO)] (M = Zr, Hf) species detected spectroscopically at low temperature.[12,13] In summary, all the species discussed in this paragraph are, despite their high oxidation states, either d-electron rich, kinetically trapped at low temperatures, or utilise ligand-to-ligand not metal-to-ligand backbonding, and they should not be confused with non-classical, cationic carbonyl complexes where the M-CO σ-bonding component dominates the bonding picture with little or no π-backbonding contributions.[14,15]

For early actinides, outside of cryogenic matrix isolation conditions[2,3] N_2 derivatives tend to be strongly activated and reduced to side-on-bound $(N_2)^{n-}$ by polymetallic-mediated reductions,[16-19] or complete cleavage to nitrides occurs.[20,21] Very few isolable, structurally characterised end-on CO, N_2, or NO actinide complexes are known,[22-29] and all terminal end-on complexes are supported by *tris*(cyclopentadienyl) ligand sets.[22-25,27-29] The backbonding in these systems stems not from metal orbitals but cyclopentadienyl ligand orbitals,[30] reminiscent of transition metal analogues,[11] or in the case of NO formal full reduction to $(NO)^{1-}$ occurs,[29] so these are quite different from the classical metal-to-ligand backbonding model.[1] Notably, all uranium complexes with end-on CO or N_2 involve electron-rich $5f^3$ uranium(III).[22-25,28] Although 5f orbitals are radially more expanded than 'core-like' 4f orbitals, they only just penetrate the valence region, so such metal-to-ligand interactions and π-acceptor ligand activation is weak, as evidenced by their reversible coordination and dominance of ligand-to-ligand backbonding. However, it should be noted that even though actinide-metallocenes represent a non-classical case of donor-acceptor bonding,[30] they fundamentally comply with the classical requirements of electron rich metal ions in a medium to low metal oxidation state.

We recently reported the synthesis of the silyl-phosphino-carbene uranium(IV) complex [U(BIPM^{TMS}){C(SiMe$_3$)(PPh$_2$)}(Cl)][Li-2,2,2-cryptand] (**1**, BIPM^{TMS} = C(PPh$_2$NSiMe$_3$)$_2$) that contains two types of covalent U=C carbene double bond.[31] In order to establish the fundamental properties of **1** we have examined its reactivity towards a wide range of substrates. Here, we report that treatment of **1** with an organo-azide produces a 5f^1 high oxidation state uranium(V)-*bis*(imido) {U(NR)$_2$}$^{1+}$ derivative. This carbene to *bis*(imido) motif transformation is unknown in carbene chemistry, but more remarkably the uranium(V)-*bis*(imido) complex that is formed is surprisingly end-on bound to a molecule of N_2 which bridges end-on to a lithium counter-ion. This isolable, crystalline complex features a +V high oxidation state metal classically backbonded to a neutral π-acceptor ligand despite formally involving an electron-poor metal with only one valence electron. This is in defiance of the well-established prerequisites for synergic donor-acceptor complexes, and it does so with an electron in a 5f-orbital, ostensibly one of least radially expanded orbitals of the Periodic Table.

Results and Discussion

Synthesis. Treatment of **1** with one equivalent of 1-adamantyl-azide (AdN$_3$) in benzene results in immediate effervescence of N_2 and the red solution turning black. After work-up blackish-red crystals of [U(BIPM^{TMS})(NAd)$_2$(μ-η^1:η^1-N$_2$)(Li-2,2,2-cryptand)] (**2**) are obtained from toluene in 28% crystalline yield (by uranium content), Scheme 1. Complex **2** is formed irrespective of whether the reaction is conducted under N_2 or Ar, suggesting that the coordinated N_2 derives from the azide. Analysis of the reaction mother liquor by NMR spectroscopy reveals that more than one uranium-containing product is formed. Unfortunately, the by-products have resisted all attempts to isolate and characterise them, but hydrolysis of the mother liquor and analysis by NMR spectroscopy and chromatographic methods reveals the presence of BIPM^{TMS}H$_2$, Me$_3$SiCH$_2$PPh$_2$, and LiCl-2,2,2-cryptand in an approximate 1:2:1 ratio. This gives mass balance for the reaction and accounts for the superficially low yield of **2**, since the theoretical maximum in a scenario where sacrificial

uranium-containing by-products form is substantially lower than 100%. The reaction that produces **2** is clearly complex and most likely involves ligand scrambling, but **2** is consistently the sole isolable uranium complex from multiple reactions.

Structural characterisation. The solid-state molecular structure of **2** was determined by X-ray crystallographic studies, Fig. 2. The salient feature of **2** is the presence of a molecule of N_2 bridging between uranium and lithium ions, the latter of which is encapsulated within a 2,2,2-cryptand ligand in an irregular six-coordinate geometry. The coordination sphere of uranium is completed by a tridentate $BIPM^{TMS}$ carbene ligand *trans* to the N_2 ligand, and two mutually *trans*-imido units resulting in a distorted octahedral geometry.

The U1-N1 distance of 2.605(8) Å is longer than the sum of single bond covalent radii of uranium and nitrogen (2.41 Å),[32] and the strongly activated U-N_2 bond length of 2.220(9) Å in $[\{(Ph)(Bu^t)N\}_3Mo(\mu\text{-}\eta^1\text{:}\eta^1\text{-}N_2)U\{N(Bu^t)(C_6H_3\text{-}3,5\text{-}Me_2)\}_3]$,[33] but, by the 3σ-criterion, compares reasonably well to the U-N distance of 2.492(10) Å reported for weakly activated $[(\eta^5\text{-}C_5Me_5)_3U(N_2)]$.[28] Interestingly, there is little variation of the U-N_α-N_β angles in those three molecules, being 175.1(7), 173.8(7), and 180°, respectively, presumably reflecting that they are all backbonded linkages no matter whether they result from metal- or ligand-to-ligand backbonded electron density. We suggest that the U1-N1 distance can be considered long as a result of weak backbonding, the fact that it resides *trans* (175.9(2)°) to the strong carbene donor of the $BIPM^{TMS}$ ligand, and that the uranium ion is bonded to several stronger donor ligands overall. The N1-N2 distance of 1.139(9) Å is elongated slightly compared to the N-N distance in free-N_2 (1.0975 Å),[1] again indicating weak backbonding, and is shorter than the 1.23(1) Å distance in $[\{(Ph)(Bu^t)N\}_3Mo(\mu\text{-}\eta^1\text{:}\eta^1\text{-}N_2)U\{N(Bu^t)(C_6H_3\text{-}3,5\text{-}Me_2)\}_3]$,[33] but is indistinguishable from the 1.120(14) Å N-N distance in $[(\eta^5\text{-}C_5Me_5)_3U(N_2)]$.[28]

The U1-N5 and U1-N6 distances of 1.906(6) and 1.897(6) Å, respectively, are typical of uranium-bis(imido) units,[34] though we note the N5-U1-N6 angle (159.1(2)°) departs substantially from linearity, presumably to avoid steric clashing between the bulky Ad and $BIPM^{TMS}$ ligand substituents. The U1-C1 distance of 2.461(7) Å in **2** compares well to the analogous distance of 2.400(3) Å in the uranium(VI)-carbene-imido-oxo complex $[U(BIPM^{TMS})(NC_6H_2\text{-}2,4,6\text{-}Me_3)(O)(DMAP)]$ (DMAP = 4-dimethylaminopyridine),[35] but considering the formal uranium(V/VI) oxidation states of these two complexes the U=C bonds are long reflecting the presence of several multiple bond donor ligands. For example, in the uranium(V)-carbene complex $[U(BIPM^{TMS})(Cl)_2(I)]$ the U=C distance is 2.268(10) Å,[36] and we suggest the long U=C bond in **2** arises from the uranium ion being electron rich from the two imido ligands and that the *bis*(imido) combination is the primary bonding motif with binding of the $BIPM^{TMS}$ being secondary.

The N2-Li1 distance of 2.008(15) Å compares well to the sum of the single bond covalent radii of nitrogen and lithium (2.04 Å),[32] and is indeed reminiscent of Li-NR_2 distances generally, suggesting that the N_2 carries partial anionic character resulting from backbonding from the $5f^1$ uranium(V) ion. During crystallographic refinement of **2** the possibility that the N_2 could be other diatomic small molecules (C_2, CN, CO, NO, O_2) or a disordered chloride was considered in detail, but is ruled out by a combination of incompatibility with the crystallographic metrical data, chemical unfeasibility of their occurrence, and the oxidation state formulation confirmed by the characterisation data below.

Spectroscopic and magnetic characterisation. The NMR spectra that could be obtained for **2**, noting its poor solubility once isolated, are well resolved and essentially within diamagnetic ranges (Supplementary Information Fig. S1-S4), however this is common for uranium(V) complexes which are weakly paramagnetic and the data for **2** are in good agreement with those of related uranium(V)-BIPM complexes.[36-38] The Raman spectrum of **2** (Supplementary Information Fig. S5)

exhibits a broad $\nu(N_2)$ absorption centred at ~1940 cm^{-1}, which compares reasonably well to a computed $\nu(N_2)$ value of 2038 cm^{-1} from a DFT analytical frequencies calculation of **2** using atomic coordinates from the experimentally determined crystal structure (see below). Additionally, it has been shown[39,40] that $\nu(N_2)$ is proportional to $d(N_2)$ to the 3/2-power as:

$$\nu(N_2) = -1840[d(N_2)]^{3/2} + 4130 \text{ (Eqn 1.)}$$

Using Eqn 1 and the N1-N2 distance of 1.139(9) Å in **2**, a $\nu(N_2)$ frequency centred at 1890 cm^{-1} is predicted, and noting that by the 3σ-criterion the N1-N2 distance spans the range 1.112-1.166 Å the $\nu(N_2)$ frequency is predicted to, and does, fall in the range 1813-1972 cm^{-1}. Considering that the N1-N2 solid-state distance is determined in close proximity to the heavy uranium and that N_2-containing molecules, including N_2 itself, frequently deviate by up to 300 cm^{-1} from predictions[39,40] based on Eqn 1, the fit for **2** is remarkably good. The $\nu(N_2)$ frequency of **2** is ~390 cm^{-1} lower (Δ) than that of free N_2 (2331 cm^{-1}) (*1*), indicating weak, but not insignificant, backbonding and activation. For comparison, the $\nu(N_2)$ frequency of $[(\eta^5\text{-}C_5Me_5)_3U(N_2)]$ is 2207 cm^{-1} (Δ = 124 cm^{-1}, $\nu(N_2)$ predicted to be 1949 cm^{-1} by Eqn 1),[28] suggesting very weak backbonding in that case, whereas the $\nu(N_2)$ frequency of $[\{(3,5\text{-}Me_2\text{-}C_6H_3)(Ad)N\}_3Mo(\mu\text{-}\eta^1\text{:}\eta^1\text{-}N_2)U\{N(Bu^t)(C_6H_3\text{-}3,5\text{-}Me_2)\}_3]$ is 1568 cm^{-1} (Δ = 763 cm^{-1}) suggesting strong backbonding in that case.[33] These spectroscopic data correlate with the observed stabilities of **2** and $[(\eta^5\text{-}C_5Me_5)_3U(N_2)]$,[28] where the latter requires a pressure of 80 psi to form, with N_2 release observed when the pressure is returned to 14.7 psi (1 atm), whereas the former forms at 1 atm pressure and does not release N_2 even when placed under dynamic vacuum (0.01 mm Hg), nor exchange with $^{15}N_2$ when refluxed in toluene under $^{15}N_2$, which instead results in decomposition to unidentifiable products and any remaining **2** shows no sign of $^{15}N_2$-incorporation. Further confirming this trend, the related carbonyl complex $[(\eta^5\text{-}C_5Me_5)_3U(CO)]$ exhibits a $\nu(CO)$ frequency that is 221 cm^{-1} lower than free CO,[25] and this compound liberates CO only after several hours under vacuum. The attenuated total reflectance infrared (ATR-IR) spectrum of **2** (Supplementary Information Fig. S6) exhibits several weak

absorptions in the range 1900-2100 cm^{-1}, but none of these could be definitively assigned as a $\nu(N_2)$ absorption, and attempts to perform ^{15}N-labelling studies proved intractable.

The ultraviolet/visible/near-infrared (UV/Vis/NIR) electronic absorption spectrum of **2** (Supplementary Information Fig. S7) is dominated by strong charge transfer bands that tail from the UV region to ~12,000 cm^{-1}. The NIR region exhibits weak (ε = 10-20 L mol^{-1} cm^{-1}) Laporte forbidden f-f absorptions in the range 5555-11,000 cm^{-1} that are characteristic of intra-configurational transitions from the ground $^2F_{5/2}$ to excited $^2F_{7/2}$ term multiplets of uranium(V).[41] These absorptions are modelled well by time-dependent density functional theory (TD-DFT), revealing that they all involve electronic promotions within the U-N_2 unit (Supporting Information Fig. S8).

The uranium(V) formulation of **2** is supported by Electron Paramagnetic Resonance (EPR) spectroscopy. The solid-state X-band EPR spectrum of **2** at 5 K (Supplementary Information Fig. S9) exhibits a resonance peak at g_z = 3.80, which is similar to the axial g_z feature of terminal uranium(V)-nitrides supported by tripodal ligands (g ~3.7);[42] as for those nitrides, no $g_{x,y}$ features are observed for **2** within the available magnetic field range, 0-18,000 Gauss, suggesting that $g_{x,y}$ < 0.4. This resonance peak is observable only below 50 K, consistent with 5f-electron character since rapid relaxation can occur due to the high orbital angular momenta of 5f-orbitals.

Unequivocal confirmation of the +V oxidation state assignment of **2** comes from variable-temperature superconducting quantum interference device (SQUID) magnetometry, Fig. 3 and Supplementary Information Fig. S10. A powdered sample of **2** exhibits a magnetic moment of 2.33 Bohr magneton units (μ_B) at 298 K (2.28 μ_B in solution), in close agreement with a theoretical magnetic moment of 2.54 μ_B for a single uranium(V) ion. Characteristic of uranium(V), the magnetic moment decreases slowly, until at 50 K (μ_{eff} = 2.04 μ_B) the magnetic moment decreases

rapidly, reaching 0.94 μ_B at 2 K since this ion is an open shell magnetic doublet at all temperatures.[41-44]

Computational characterisation. In order to probe the nature of the bonding in **2** we performed DFT calculations. In general, the computed bond lengths and angles of the geometry optimised structure are within 0.05 Å and 2° of the experimental crystal structure. However, the U1-N1 distance of 2.439 Å in the geometry optimised gas-phase structure is ~0.16 Å shorter than the distance in the experimental solid-state crystal structure. Furthermore, inspection of a space filling representation of **2** (Supplementary Information Fig. S11) clearly shows that the N_2-Li-2,2,2-cryptand fragment could approach closer to the U(BIPM^{TMS})(NAd)$_2$ unit of **2** without any obvious steric clashing. Moreover, an analytical frequencies calculation on the geometry optimised coordinates computes a N_2 stretch of 1712 cm^{-1}, which does not compare well with the experimentally determined value.

In order to probe this further, we performed potential energy surface scans along the U1-N1 vector, both on the full molecule and on a simplified model (**2 core**) in which phenyl and adamantyl groups are replaced with methyl groups, $SiMe_3$ is substituted for SiH_3 and only the coordinating atoms of the cryptand are retained (Supplementary Information Fig. S12). Several levels of theory have been employed, and the results are summarised in Fig. 4. DFT (PBE) scans give minimum energies between 2.35-2.41 Å, whereas Hartree-Fock (HF) scans show minima at around 2.50 Å. Second-order Møller–Plesset perturbation theory (MP2) calculations yield similar conclusions to HF. Restricted active space-self consistent field (RASSCF) calculations have also been performed; the choice of active space is discussed in detail in the Supplementary Information, and the natural orbitals are shown in Fig. S13 and their occupancies, at each point in the scan, in Table S1. These calculations give an energy minimum at 2.56 Å, with a significantly shallower potential compared to the already rather shallow HF and DFT scans; the point at 2.61 Å is only 0.80 kJ mol^{-1} higher in

energy. It may be that including further correlation shifts the minimum even closer to the crystal structure geometry, as may the additional sterics of the full molecule. We note that the very shallow potentials shown in Fig. 4 are well within the range of crystal packing forces,[45] and hence conclude that the discrepancy of the experimental vs computed U1-N1 distance is either the result of solid-state crystal packing effects that are not accounted for in gas phase calculations and/or correlation energy effects not well described by DFT.

Noting the experimental vs computed U1-N1 discrepancy, to obtain an experimentally relevant description of the electronic structure of **2** DFT studies were performed using the crystallographic coordinates and not geometry optimised ones. The good agreement of TD-DFT and analytical frequencies calculations using those coordinates to experimental observations provides validation of this approach. The computed MDC-q charges on the U1, C1, Li1, and N_2 units are +3.36, –2.14, +0.66, and –0.51. In a purely ionic bonding situation these values would be +5, –2, +1, and 0, so the computed data reflect charge donation to the U1 and Li1 ions from the ligands and backbonding from uranium to the N_2 ligand. Consistent with this, the spin densities on U1 and N_2 unit are –0.6 and –0.51, confirming transfer of ~0.5 of an electron from the formal $5f^1$ U1 to N_2. In further support of this backbonding picture, the U1-N1 and N_2 computed Nalewajski-Mrozek bond orders are 0.66 and 2.75, respectively, showing a weak U-N_2 backbond and modest reduction of the N_2 bond order (3 in free N_2). As suggested by the U1-C1 distance, the U1-C1 bond is poorly developed with a bond order of 0.92, reflecting the presence of the two imido groups with U1-N5 and U1-N6 bond orders of 2.57 and 2.59 that are consistent with strong triple bonds. For comparison the U1-N3 and U1-N4 bond orders are 0.77 and 0.79, respectively, and a highly polar N2-Li1 interaction is confirmed by a computed bond order of 0.13.

The highest occupied Kohn-Sham molecular orbital (HOMO) of **2** is the U-N_2 backbond, Fig. 5. This is consistent with the formal $5f^1$ +V oxidation state of the uranium ion in **2** and backbonding to

N_2. The U-$C_{carbene}$ double bond is principally represented by HOMO−1 (π) and HOMO−2 (σ) (Supplementary Information Fig. S14). The U-N_{imido} bonding interactions are represented by HOMO−3 to HOMO−11, but these MOs are extensively mixed. Therefore, in order to obtain a clearer and chemically more intuitive description of the bonding in **2** we turned to Natural Bond Orbital (NBO) theory.

NBO calculations on **2** (Supplementary Information Fig. S15) reveal one U-N_2 backbonding interaction that is composed of 31% U1 and 69% N1 character. As expected, the N component is essentially pure 2p-orbital character from the π*-orbital manifold of N_2 and the uranium contribution is 95% 5f and 5% 6d character. The N_2 lone pair donation to U is described in an NBO of exclusively N-character (62% 2s and 38% 2p character), in-line with its dative, and weak, nature. Confirming analysis of the Kohn-Sham electronic structure, NBO returns a $\sigma^2\pi^2$ U-C double bond interaction and also two $\sigma^2\pi^2\pi^2$ U-N_{imido} triple bond interactions. The U=C bonds are quite polar, being composed of 10% uranium and 90% carbon character with the uranium component dominated by 5f character (80:20 5f:6d), whereas the U-N_{imido} bonds have 20% uranium and 80% nitrogen character with a 5f:6d ratio of 70:30.

DFT and NBO methods are orbital-based, and in order to probe the chemical bonding in **2** in an alternative way we examined the topology of the electron density using Quantum Theory of Atoms in Molecules (QTAIM). A U1-N1 3,−1 bond critical point (BCP) was found, with an electron density $\rho(r)$ of 0.04 e $bohr^{-3}$. In QTAIM analysis covalent bond tends to have $\rho(r) > 0.1$ so the value for **2** is consistent with a polar bonding interaction, which is also reflected by the total energy density $H(r)$ (–0.01) at the BCP. The presence of the backbond is unequivocally confirmed by examination of the bond ellipticity, $\varepsilon(r)$. Single (σ^2, e.g. H_3CCH_3) and triple ($\sigma^2\pi^2\pi^2$, e.g. HC≡CH) bonds exhibit spherical distributions of electron density around the bond path at the BCP and so $\varepsilon(r) \sim 0$, however double bonds ($\sigma^2\pi^2$, e.g. $H_2C{=}CH_2$) are asymmetric and so $\varepsilon(r) > 0$, being 0.45 for

$H_2C{=}CH_2$.[46] Here, the ε(r) value for the U1-N1 bond in **2** is 0.39, confirming a single π-backbond. For comparison, the U1-C1, av. U-N_{imido}, and N1-N2 ρ(r)/*H*(r)/ε(r) data are 0.08/–0.03/0.24, 0.20/–0.14/0.01, and 0.6/–0.91/0.01, respectively. Taken together with all the other data, the consistent picture that emerges is a U-N_2 donor-acceptor interaction with a π-backbond that only weakly activates the N≡N triple bond, and polarised covalent U-$C_{carbene}$ double and U-N_{imido} triple bonds.

Discussion. Complex **2** violates the traditional requirements of synergic, donor-acceptor metal-to-ligand interactions. Furthermore, this situation arises in an electron-poor, high oxidation state complex, involving the poor π-acceptor N_2, utilising a single electron in a 5f-orbital, which is one of the least radially expanded orbitals, and therefore one of the least likely candidates for this scenario to occur. So how can this situation arise? We propose two factors that may be responsible. The heterobimetallic uranium-lithium combination may cooperatively assist in trapping the N_2, and certainly heteropolymetallic cooperative effects are increasingly being recognised as crucial to binding and activating N_2 in heterogeneous Haber Bosch chemistry and in homogeneous molecular analogues.[1,47] Recognising that electron-poor, high oxidation state metals can also backbond to N_2 by tuning the ligand environment could have implications for N_2-activation chemistry given the vast scale that industrial Haber Bosch and biomimetic nitrogenase processes operate on.[48] The uranium ion in **2** is bonded to two imido ligands and the tridentate $BIPM^{TMS}$ carbene ligand. We suggest that with at least three strong multiply bonded π-donor ligands, the formally electron-poor $5f^1$ uranium ion in **2** is evidently uncommonly capable of engaging in π-backbonding even to a poor π-acceptor ligand. Uranium(V) is usually considered to be quite oxidising,[41] but here the uranium is in such an electron rich ligand environment that it is now essentially reducing in nature. The isolation of crystalline **2**, and the prior report of meta-stable $[OsO_2(CO)_4]^{2+}$ (reference 10) that contains one less metal-ligand multiple bond linkage than stable **2**, suggests that isolable complexes that breach the

basic rules of the classical donor-acceptor bonding model might be realised more widely by electron-poor metals when coordinated by very electron-rich ancillary ligands.

Conclusions and Summary

To conclude, we have found that reaction of a uranium-carbene complex with an organo-azide results in isolation of a crystalline uranium(V)-*bis*(imido)-dinitrogen complex. To the best of our knowledge this carbene to *bis*(imido) motif transformation is unprecedented in carbene chemistry, yet more remarkably the uranium(V)-*bis*(imido) complex that is formed is surprisingly end-on bound to a molecule of N_2 which bridges end-on to a lithium counter-ion. This isolable, crystalline complex features a +V high oxidation state metal classically backbonded to a neutral π-acceptor ligand despite formally involving an electron-poor metal with only one valence electron and a very poor π-acceptor ligand. This is in defiance of the well-established prerequisites for synergic donor-acceptor complexes, and it does so with an electron in a 5f-orbital, ostensibly one of less radially expanded orbitals of the Periodic Table. We propose that this scenario arises due to a combination of cooperative heterobimetallic effects and that the uranium ion in this complex is unusually electron-rich to the point that a usually oxidising metal centre is now reducing in nature. This suggests that with suitable ancillary ligands isolable complexes that breach the basic rules of the classical donor-acceptor bonding model might be realised more widely by electron-poor metals when coordinated by very electron-rich ancillary ligands. Lastly, N_2-activation chemistry usually relies on the use of low-valent reducing metal ions, but this work suggests that in the suitable situations high oxidation state metals could also play a role in the binding and activation of dinitrogen.

Acknowledgements

We gratefully acknowledge funding and support from the UK Engineering and Physical Sciences Research Council (grants EP/M027015/, and EP/P001386/1), European Research Council (grant

CoG612724), Royal Society (grant UF110005), the National EPSRC UK EPR Facility, The University of Manchester, and the UK National Nuclear Laboratory. B.E.A and N.K are also grateful to the University of Manchester for computational resources and associated support services from the Computational Shared Facility.

Accession Codes

The X-ray crystallographic data for **2** have been deposited at the Cambridge Crystallographic Data Centre (CCDC), under deposition number CCDC 1869009. These data can be obtained free of charge from The Cambridge Crystallographic Data Centre (www.ccdc.cam.ac.uk/data_request/cif).

Author Contributions

E.L. and J.B. prepared and characterised the compound and its precursors. B.E.A. and N.K. performed the energy-scan calculations and analysed the results. E.L., A.J.W., I.J.V.-Y., and G.F.S.W. collected, solved, refined, and analysed the crystallographic data. E.L., L.R.D., J.D.C., and P.C. recorded and interpreted the Raman data. F.T. recorded and interpreted the EPR data. S.T.L. originated the central idea, supervised the work, analysed the data, performed the DFT, NBO, and QTAIM calculations and analysed the results, and wrote the manuscript with contributions from all authors.

Additional Information

Supplementary information and chemical compound information are available in the online version of the paper. Reprints and permissions information is available at www.nature.com/reprints. Correspondence and requests for materials should be addressed to S.T.L.

Competing Financial Interests

The authors declare no competing financial interests.

References

1. Fryzuk, M. D. & Johnson, S. A. The continuing story of dinitrogen activation. *Coord. Chem. Rev.* **200-202**, 379-409 (2000).
2. Kushto, G. P., Souter, P. F. & Andrews, L. An infrared spectroscopic and quasirelativistic theoretical study of the coordination and activation of ninitrogen by thorium and uranium atoms. *J. Chem. Phys.* **108**, 7121 (1998).
3. Andrews, L., Wang, X., Gong, Y., Vlaisavljevich, B. & Gagliardi, L. Infrared spectra and electronic structure calculations for the $NUN(NN)_{1-5}$ and $NU(NN)_{1-6}$ complexes in solid argon. *Inorg. Chem.* **52**, 9989-9993 (2013).
4. Burford, R. J. & Fryzuk, M. D. Examining the relationship between coordination mode and reactivity of dinitrogen. *Nat. Rev. Chem.* **1**, 0026 (2017).
5. Dell'Amico, D. B., Calderazzo, F., Marchetti, F. & Merlino, S. Synthesis and molecular structure of $[Au_4Cl_8]$, and the isolation of $[Pt(CO)Cl_5]^-$ in thionyl chloride. *J. Chem. Soc. Dalton Trans.* 2257-2260 (1982).
6. Bernhardt, E. & Preetz, W. Sythesis and spectroscopic characterization of fluorocarbonylosmates, normal coordinate analysis and crystal structure of *fac*-$[OsF_3Br_2(CO)]^{2-}$. *Z. Anorg. Allg. Chem.* **624**, 694-700 (1998).
7. Höhling, M. & Preetz, W. Synthesis and crystal structure of tetraphenylarsonium pentachlorocarbonylosmate(IV), $(Ph_4As)[OsCl_5(CO)]$. *Z. Naturforsch.* **B52**, 978-980 (1997).
8. Wovchko, E. A. & Yates, J. T. Activation of O_2 on a photochemically generated Rh^I site on an Al_2O_3 surface: low temperature O_2 dissociation and CO oxidation. *J. Am. Chem. Soc.* **120**, 10523-10527 (1998).
9. Crayston, J. A., Almond, M. J., Downs, A. J., Poliakoff, M. & Turner, J. J. Formation of *trans*-$M(O)_2(CO)_4$ (M = Mo and W): intermediates in the photooxidation of matrix-isolated $M(CO)_6$. *Inorg. Chem.* **23**, 3051-3056 (1984).

10. Bernhardt, E., Willner, H., Jonas, V., Thiel, W., & Aubke, F. The tetrakis(carbonyl)dioxoosmium(VI) cation: *trans*-$[OsO_2(CO)_4]^{2+}$. *Angew. Chem. Int. Ed.* **39**, 168-171 (2000).

11. Malischewski, M., Seppelt, K., Sutter, J., Munz, D. & Meyer, K. A ferrocene-based dicationic iron(IV) carbonyl complex. *Angew. Chem. Int. Ed.* **57**, 14597-14601 (2018).

12. Marsella, J. A., Curtis, C. J., Bercaw, J. E. & Caulton, K. G. Low-temperature infrared study of d^0 carbonyl complexes. *J. Am. Chem. Soc.* **102**, 7244-7246 (1980).

13. Guram, A. S., Swenson, D. C. & Jordan, R. F. Synthesis and characterization of $Cp_2Zr(CH\{Me\}\{6\text{-ethylpyrid-2-yl}\})(CO)^+$, a d^0 metal alkyl carbonyl complex. Coordination chemistry of the four-membered azazirconacycle $Cp_2Zr(\eta^2\text{-}C,N\text{-}CH\{Me\}\{6\text{-ethylpyrid-2-yl}\})^+$. *J. Am. Chem. Soc.* **114**, 8991-8996 (1992).

14. Hurlburt, P. K. *et al*. Nonclassical metal carbonyls: $[Ag(CO)]^+$ and $[Ag(CO)_2]^+$. *J. Am. Chem. Soc.* **116**, 10003-10014 (1994).

15. Lupinetti, A. J., Frenking, G. & Strauss, S. H. Nonclassical metal carbonyls: appropriate definitions with a theoretical justification. *Angew. Chem. Int. Ed.* **37**, 2113-2116 (1998).

16. Roussel, P. & Scott, P. Complex of dinitrogen with trivalent uranium. *J. Am. Chem. Soc.* **120**, 1070-1071 (1998).

17. Cloke, F. G. N. & Hitchcock, P. B. Reversible binding and reduction of dinitrogen by a uranium(III) pentalene complex. *J. Am. Chem. Soc.* **124**, 9352 (2002).

18. Mansell, S. M., Kaltsoyannis, N. & Arnold, P. L. Small molecule activation by uranium tris(aryloxides): experimental and computational studies of binding of N_2, coupling of CO, and deoxygenation insertion of CO_2 under ambient conditions. *J. Am. Chem. Soc.* **133**, 9036-9051 (2011).

19. Mansell, S. M., Farnaby, J. H., Germeroth, A. I. & Arnold, P. L. Thermally stable uranium dinitrogen complex with siloxide supporting ligands. *Organometallics* **32**, 4214-4222 (2013).

20. Korobkov, I., Gambarotta, S. & Yap, G. P. A. A highly reactive uranium complex supported by the calix[4]tetrapyrrole tetraanion affording dinitrogen cleavage, solvent deoxygenation, and polysilanol depolymerisation. *Angew. Chem. Int. Ed.* **41**, 3433-3436 (2002).

21. Falcone, M., Chatelain, L., Scopelliti, R., Zivkovic, I. & Mazzanti, M. Nitrogen reduction and functionalization by a multimetallic uranium nitride complex. *Nature* **547**, 332-335 (2017).

22. Brennan, J. G., Andersen, R. A. & Robbins, J. L. Preparation of the first molecular carbon monoxide complex of uranium, $(Me_3SiC_5H_4)_2UCO$. *J. Am. Chem. Soc.* **108**, 335-336 (1986).

23. Parry, J., Carmona, E., Coles, S. & Hursthouse, M. Synthesis and single crystal X-ray diffraction study on the first isolable carbonyl complex of an actinide, $(C_5Me_4H)_3U(CO)$. *J. Am. Chem. Soc.* **117**, 2649-2650 (1995).

24. Del Mar Conejo, M., Parry, J. S., Carmona, E., Schultz, M., Brennan, J. G., Beshouri, S. M., Andersen, R. A., Rogers, R. D., Coles, S. & Hursthouse, M. B. Carbon monoxide and isocyanide complexes of trivalent uranium metallocenes. *Chem. Eur. J.* **5**, 3000-3009 (1999).

25. Evans, W. J,. Kozimor, S. A., Nyce, G. W. & Ziller, J. W. Comparative reactivity of sterically crowded nf^3 $(C_5Me_5)_3Nd$ and $(C_5Me_5)_3U$ complexes with CO: formation of a nonclassical carbonium ion versus an f element metal carbonyl complex. *J. Am. Chem. Soc.* **125**, 13831-13835 (2003).

26. Castro-Rodriguez, I. & Meyer, K. Carbon dioxide reduction and carbon monoxide activation employing a reactive uranium(III) complex. *J. Am. Chem. Soc.* **127**, 11242-11243 (2005).

27. Langeslay, R. R., Chen, G. P., Windorff, C. J., Chan, A. K., Ziller, J. W., Furche, F. & Evans, W. J. Synthesis, structure, and reactivity of the sterically crowded Th^{3+} complex $(C_5Me_5)_3Th$ including formation of the thorium carbonyl, $[(C_5Me_5)_3Th(CO)][BPh_4]$. *J. Am. Chem. Soc.* **139**, 3387-3398 (2017).

28. Evans, W. J., Kozimor, S. A. & Ziller, J. W. A monometallic f element complex of dinitrogen: $(C_5Me_5)_3U(\eta^1\text{-}N_2)$. *J. Am. Chem. Soc.* **125**, 14264-14265 (2003).

29. Siladke, N. A., Meihaus, K. R., Ziller, J. W., Fang, M., Furche, F., Long, J. R. & Evans, W. J. Synthesis, structure, and magnetism of an f element nitrosyl complex, $(C_5Me_4H)_3UNO$. *J. Am. Chem. Soc.* **134**, 1243-1249 (2012).

30. Maron, L., Eisenstein, O. & Andersen, R. A. The bond between CO and Cp'_3U in $Cp'_3U(CO)$ involves back-bonding from the Cp'_3U ligand-based orbitals of π-symmetry, where Cp' represents a substituted cyclopentadienyl ligand *Organometallics* **28**, 3629-3635 (2009).

31. Lu, E., Boronski, J. T., Gregson, M., Wooles, A. J. & Liddle, S. T. Silyl-phosphino-carbene complexes of uranium(IV). *Angew. Chem. Int. Ed.* **57**, 5506-5511 (2018).

32. Pyykkö, P. Additive covalent radii for single-, double-, and triple-bonded molecules and tetrahedrally bonded crystals: A summary. *J. Phys. Chem. A* **119**, 2326-2337 (2015).

33. Odom, A. L., Arnold, P. L. & Cummins, C. C. Heterodinuclear uranium/molybdenum dinitrogen complexes. *J. Am. Chem. Soc.* **120**, 5836-5837 (1998).

34. Hayton, T. W., Boncella, J. M., Scott, B. L., Palmer, P. D., Batista, E. R. & Hay, P. J. Synthesis of imido analogs of the uranyl ion. *Science* **310**, 1941-1943 (2005).

35. Lu, E., Cooper, O. J., McMaster, J., Tuna, F., McInnes, E. J. L., Lewis, W., Blake, A. J. & Liddle, S. T. Synthesis, Characterization, and Reactivity of a Uranium(VI) Carbene Imido Oxo Complex. *Angew. Chem. Int. Ed.* **53**, 6696-6700 (2014).

36. Cooper, O. J., Mills, D. P., McMaster, J., Moro, F., Davies, E. S., Lewis, W., Blake, A. J. & Liddle, S. T. Uranium-Carbon Multiple Bonding: Facile Access to the Pentavalent Uranium Carbene $[U\{C(PPh_2NSiMe_3)_2\}(Cl)_2(I)]$ and Comparison of U^V=C and U^{IV}=C Double Bonds. *Angew. Chem. Int. Ed.* **50**, 2383-2386 (2011).

37. Mills, D. P. *et al.* Synthesis of a uranium(VI)-carbene: reductive formation of uranyl(V)-methanides, oxidative preparation of a $[R_2C=U=O]^{2+}$ analogue of the $[O=U=O]^{2+}$ uranyl ion ($R = Ph_2PNSiMe_3$), and comparison of the nature of U^{IV}=C, U^V=C and U^{VI}=C double bonds. *J. Am. Chem. Soc.* **134**, 10047-10054 (2012).

38. Cooper, O. J. *et al.* The nature of the U=C bond: Pushing the stability of high oxidation state uranium carbenes to the limit. *Chem. Eur. J.* **19**, 7071-7083 (2013).

39. Cohen, J. D., Mylvaganam, M., Fryzuk, M. D. & Loehr, T. M. Resonance Raman studies of dinuclear zirconium complexes with a bridging dinitrogen ligand. Possible N_2-coordination models for nitrogenase. *J. Am. Chem. Soc.* **116**, 9529-9534 (1994).

40. Laplaza, C. E. *et al*. Dinitrogen cleavage by three-coordinate molybdenum(III) complexes: mechanistic and structural data. *J. Am. Chem. Soc.* **118**, 8623-8638 (1996).

41. Liddle, S. T. The Renaissance of Non-Aqueous Uranium Chemistry. *Angew. Chem. Int. Ed.* **54**, 8604-8641 (2015).

42. King, D. M., Cleaves, P. A., Wooles, A. J., Gardner, B. M., Chilton, N. F., Tuna, F., Lewis, W., McInnes, E. J. L. & Liddle, S. T. Molecular and Electronic Structure of Terminal and Alkali Metal-Capped Uranium(V)-Nitride Complexes. *Nat. Commun.* **7**, 13773 (2016).

43. Castro-Rodríguez, I. & Meyer, K. Small molecule activation at uranium coordination complexes: control of reactivity *via* molecular architecture. *Chem. Commun.* 1353-1368 (2006).

44. Kindra, D. R. & Evans, W. J. Magnetic susceptibility of uranium complexes. *Chem. Rev.* **114**, 8865-8882 (2014).

45. Minasian, S. G., Krinsky, J. L. & Arnold, J. Evaluating f-element bonding from structure and thermodynamics. *Chem. Eur. J.* **17**, 12234-12245 (2011).

46. Bader, R. F. W., Slee, T. S., Cremer, D. & Kraka, E. Description of conjugation and hyperconjugation in terms of electron distributions. *J. Am. Chem. Soc.* **105**, 5061-5068 (1983).

47. MacLeod, K. C. & Holland, P. L. Recent developments in the homogeneous reduction of dinitrogen by molybdenum and iron. *Nat. Chem.* **5**, 559-565 (2013).

48. S. L. Foster, S. I. Perez Bakovic, R. D. Duda, S. Maheshwari, R. D. Milton, S. D. Minteer, M. J. Janik, J. N. Renner, L. F. Greenlee, *Nat. Cat.* **1**, 490 (2018).

Figures and Schemes:

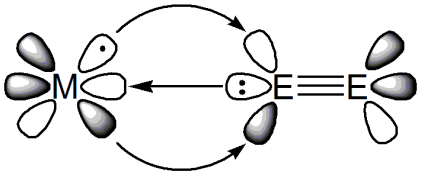

Donor-acceptor requirements:
Transition Metal
Low- or mid-oxidation state
One or more d-electrons
Spatial reach of d-orbitals

Ligand
Electron lone pair to donate to metal
Accessible π* orbital for back-bonding

This work
High oxidation state metal
5f-orbital electron

Figure 1. The classical synergic, donor-acceptor bonding model for a transition metal and a neutral diatomic E≡E (N≡N or C≡O) π-acceptor ligand complex and comparison to findings of this work.

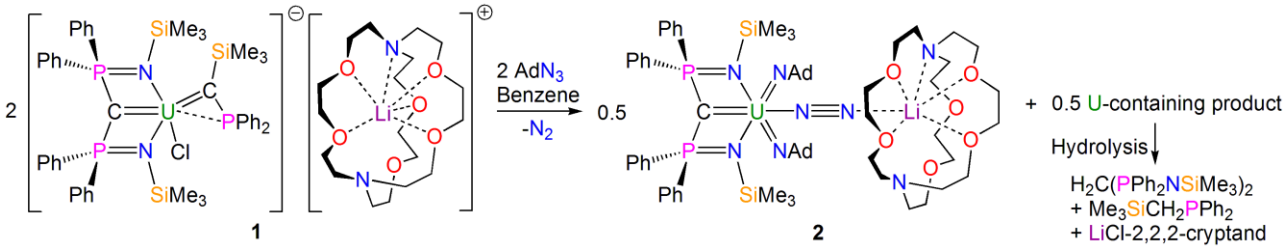

Scheme 1. Synthesis of [U(BIPM^{TMS})(NAd)$_2$(μ-η^1:η^1-N$_2$)(Li-2,2,2-cryptand)] (**2**) from [U(BIPM^{TMS}){C(SiMe$_3$)(PPh$_2$)}(Cl)][Li-2,2,2-cryptand] (**1**) and 1-adamantyl-azide (AdN$_3$).

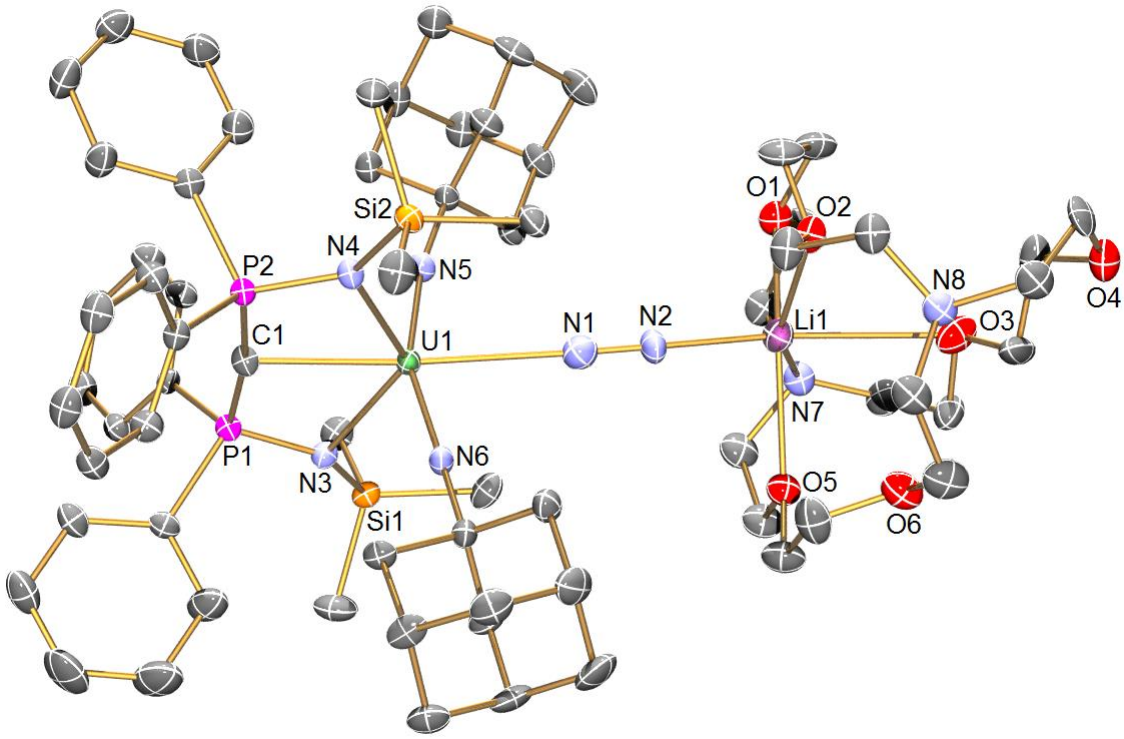

Figure 2. Molecular structure of [U(BIPM^{TMS})(NAd)$_2$(μ-η^1:η^1-N$_2$)(Li-2,2,2-cryptand)] (**2**) at 150 K with 40% probability ellipsoids. Selected distances (Å) and angles (°) are U1-N1, 2.605(8); U1-C1, 2.461(7); U1-N3, 2.452(6); U1-N4, 2.451(6); U1-N5, 1.906(6); U1-N6, 1.897(6); N1-N2, 1.139(9); N2-Li1, 2.008(15); C1-U1-N1, 175.9(2); U1-N1-N2, 175.1(7); N1-N2-Li1, 175.4(8); P1-C1-P2, 169.9(5); N5-U1-N6, 159.1(2); N3-U1-N4, 127.26(19); C1-U1-N5 99.9(3); C1-U1-N6, 101.0(2); N1-U1-N5 78.2(2); N1-U1-N6 81.0(2).

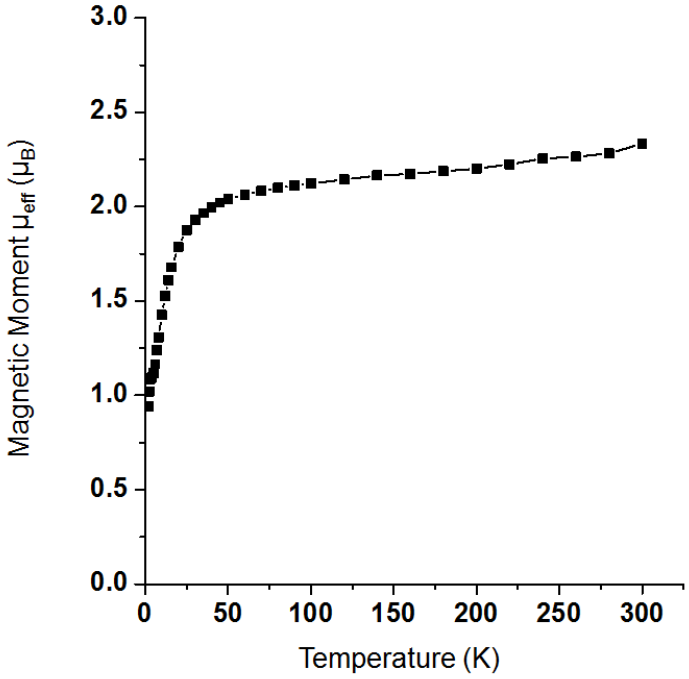

Figure 3. Temperature-dependent SQUID magnetisation data for **2** measured over the temperature range 1.8 to 300 K. The line is a guide to the eye only.

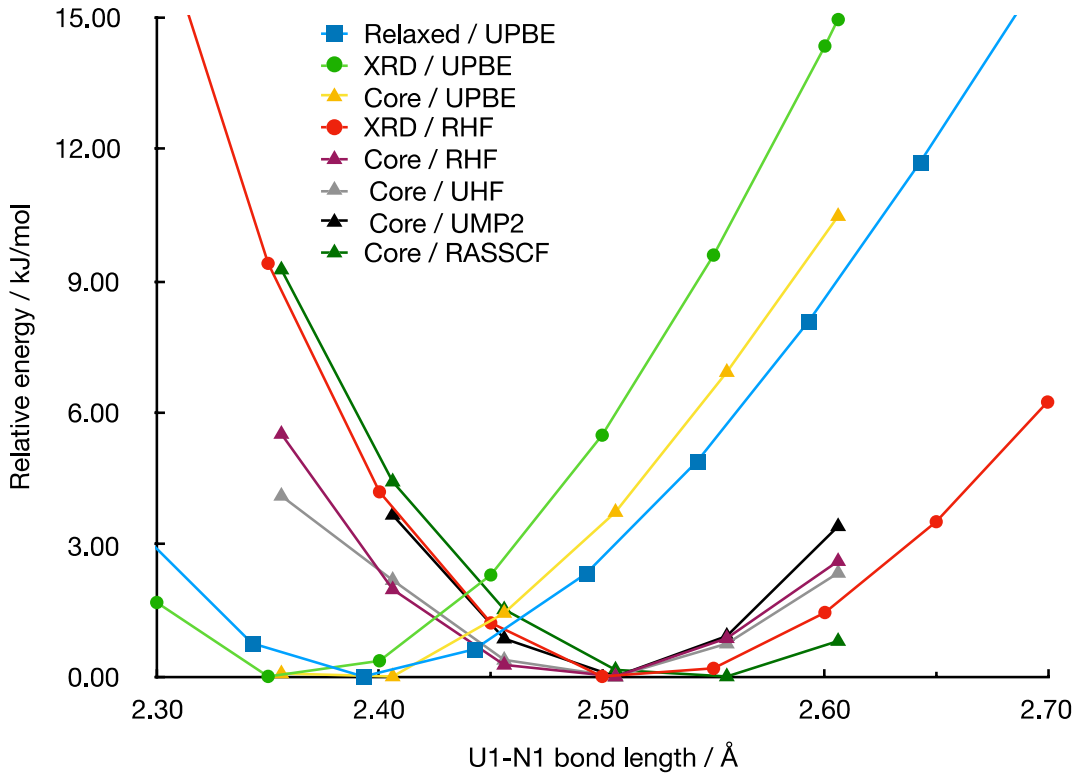

Figure 4. Relative energy (kJ mol^{-1}) vs U1-N1 distance (Å). 'XRD' and 'Relaxed' calculations are on the full molecule **2**; 'Core' is the model shown in Fig. S12 of the Supporting Information (**2 core**). All scans are rigid, *i.e.* in which all the geometric parameters of the non-hydrogen atoms are frozen, other than the U1-N1 distance, except the Relaxed / UPBE scan, in which all other geometric parameters are optimised at each point. For the rigid scans on **2 core**, the hydrogen atom positions are optimised at each point of the scan.

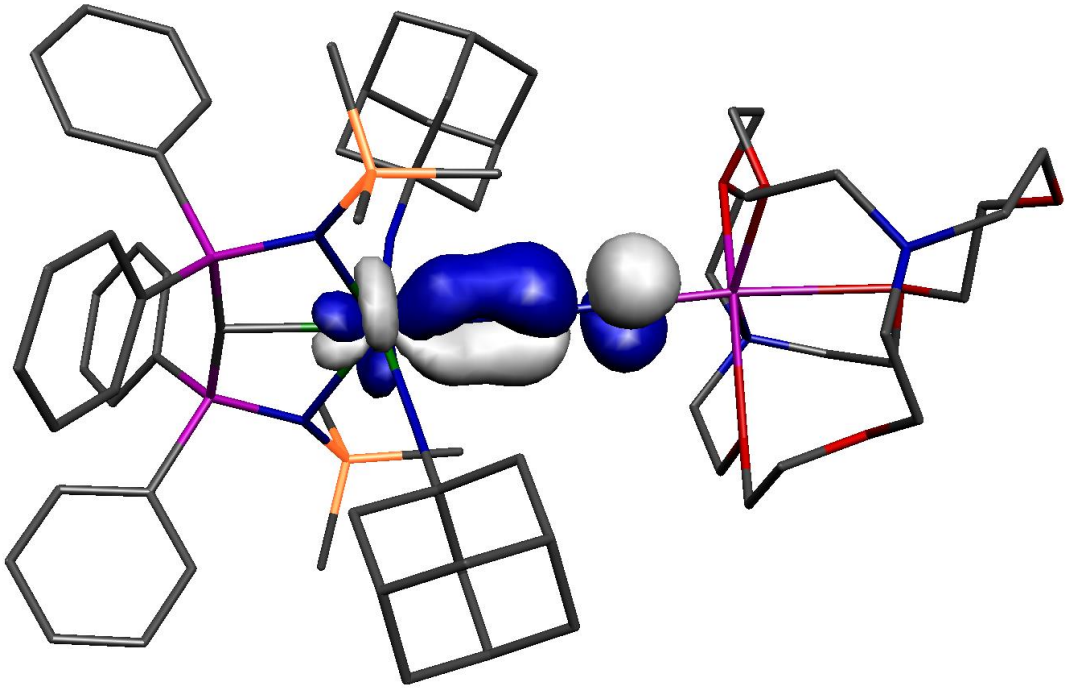

Figure 5. The singularly-occupied, α-spin highest occupied Kohn-Sham molecular orbital (338a, –1.715 eV) of **2** representing the U-N_2 backbonding interaction. Hydrogen atoms are omitted for clarity.